ARTICLE

Synthesis, Characterization, and Manipulation of Nitrogen-Doped Carbon Nanotube Cups

Brett L. Allen, Padmakar D. Kichambare,[†] and Alexander Star*

Department of Chemistry, University of Pittsburgh and the National Energy Technology Laboratory, Pittsburgh, Pennsylvania. [†]Current Address: Department of Materials Science and Engineering, Carnegie Mellon University, Pittsburgh, Pennsylvania.

ABSTRACT Isolated, carbon nanotube cups with diameters of 12−40 nm have been synthesized by chemical vapor deposition through incorporation of nitrogen atoms into graphitic carbon structure and subsequent mechanical separation. Incorporation of nitrogen affords carbon nanotube cups with a unique composition comprising multiwalled, graphitic lattice with nitrogen groups on the exterior rim and hollow interior cavities. These nanostructures demonstrate the ability to participate in hydrogen bonding because of nitrogen functionalities on their open edges. Furthermore, reaction with these nitrogen functionalities results in the coupling of gold nanoparticles (GNPs) to the open rim of carbon nanotube cups. Through atomic force microscopy manipulation and adhesion force measurements, we compare the mobility of these structures on a hydrophilic surface before and after GNP coupling. Understanding of these forces will aid in useful nanostructure assembly for energy and biomedical applications.

KEYWORDS: atomic force microscopy · carbon nanotubes · chemical vapor deposition · gold nanoparticles

*Address correspondence to astar@pitt.edu.

Received for review June 10, 2008 and accepted August 07, 2008.

10.1021/nn800355v CCC: $40.75

Recent development of carbon nanostructures has drawn much attention in a multitude of fields owing to their intrinsic structure, mechanical and electrical properties, and compatibility with biologically significant systems. Interest in such systems has branched out from carbon fullerenes[1] and carbon nanotubes[2] toward other novel carbon nanomaterials such as graphitic onions,[3] cones,[4] nanohorns,[5] nanohelices,[6] nanobarrels,[7] and graphene.[8] All of these unique carbon nanomaterials show promising capabilities for applications in electronic sensors, as catalyst support, energy storage, and drug delivery.[9]

Of particular interest is the design and implementation of hollow nanostructures for utilization of their inherent cavities. For instance, it has been highly desirable to tailor nanostructures for the specific task of drug delivery and biomedical applications.[10,11] Initial studies have thus utilized the interior cavities of multiwalled carbon nanotubes for biomedical applications through ferromagnetic filling.[12] Such structures are promising for medical treatments including magnetically guided hypothermia.[12] Furthermore, nitrogen-doped cuplike structures have been proposed for applications as electrodes for probing DNA nucleotides.[13] These types of structures are also valuable for energy applications.[14] Inherent cavities create an ideal medium for hydrogen[15,16] and lithium storage[17] and utilization for field emission.[18]

To pursue the continuing progress of such materials, we have synthesized and probed hollow, graphitic nanomaterials, nitrogen-doped carbon nanotube cups, otherwise known as carbon nanobells.[19] These structures are synthesized and then characterized by a variety of microscopy techniques. In these structures, nitrogen atoms are incorporated into graphitic structure on the edges as pyridine-like nitrogen and in the interior, where nitrogen substitutes carbon atoms.[20−22] In this study, we test the reactivity of the nitrogen functionalities in terms of their interactions with functionalized surfaces and by their conjugation with gold nanoparticles (GNPs). AFM manipulation and adhesion measurements reveal strong hydrogen bonding between hydrophilic surfaces and unmodified cups that can be alleviated by GNP coupling, thus enhancing their mobility on the surfaces.

RESULTS AND DISCUSSION

Nanotube cups were synthesized using chemical vapor deposition (CVD) from liquid carbon/nitrogen precursors. Specifically, a mixture of EtOH, ferrocene, and MeCN was injected at a rate of 5 mL/hr, using H_2 and Ar carrier gases into a CVD furnace at 950 °C for one hour. Thermal decomposition of this mixture of nitrogen and hydrocarbon precursors over an *in situ* generated iron catalyst results in carbon nanotube cup growth on a quartz plate inside the reactor.

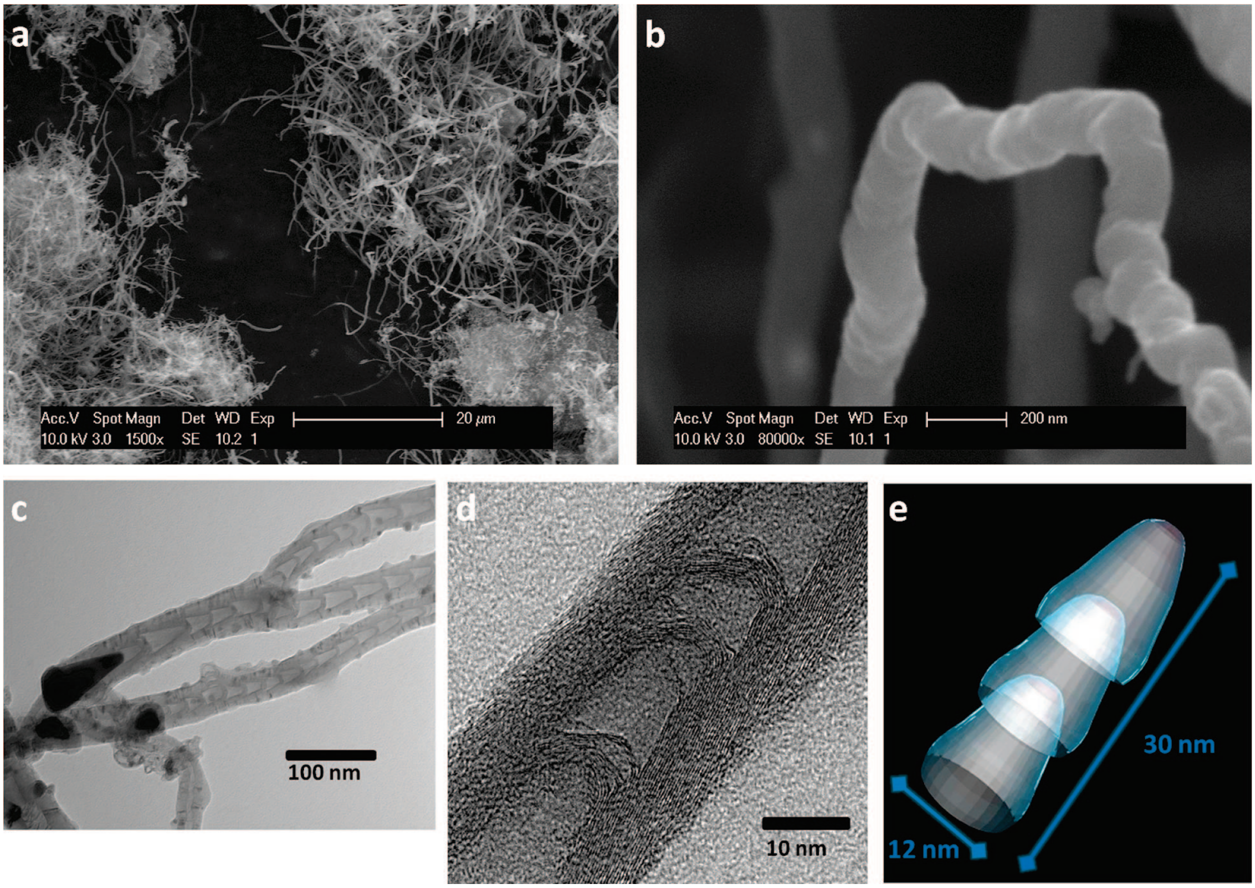

Figure 1. Synthesis of stacked nitrogen-doped carbon nanotube cups. (a,b) SEM images of as-prepared cups. (c) TEM image reveals that fibers consist of stacked cups. (d) High resolution energy-filtered TEM image of stacked, multiwalled cups. (e) Translucent schematic structural model illustrating orientation of cups with respect to nearest neighbor.

Approximately 2−3 mg (∼50% yield) of the as-prepared graphitic product was isolated as a black film layered on the quartz plate, which was peeled off with the aid of a razor blade. Scanning electron microscopy (SEM) reveals that this material is fibrous (Figure 1a). The fibers, typically 1−4 μm long and diameters ranging from 12 to 40 nm, appear as a thick carpet under low magnification. At higher magnification, an individual fiber appears with inherent "kinks" and twists along the tubular axis (Figure 1b). We used transmission electron microscopy (TEM) to make a closer examination of the fibers and elucidate their growth process. The TEM image (Figure 1c) reveals that fibers are composed of stacked cups with diameters which are defined by the size of iron catalyst nanoparticles (dark spots in the image) as seen in the case of two nanoparticles merging into one. The Fe catalyst particle is shown undergoing compression strain, which also contributes to the stacked nature of the cups, as the catalyst is ejected to form a new cup. Individual nanotube cups thus grow as conical, self-contained stacks to create an individual fiber. Their conical structure, caused by nitrogen doping at the open-edge of the nanotube cup, has been theoretically and spectroscopically examined and found to be highly dependent on the nitrogen concentration during the growth process.[23,24] This growth mechanism and structure[25] is similar to what has already been shown previously with the growth of bamboo-like carbon nanotubes.[26] High-resolution transmission electron microscopy (HRTEM) reveals the intricate lattice structure (Figure 1d). Additionally, N-doping of the carbon nanotube cup lattice was determined at 2−7% by electron energy loss spectroscopy (EELS) (Supporting Information). As with multiwalled carbon nanotubes where all lattice walls are parallel along the longitudinal axis, carbon nanotube cups deviate from this general schematic. The walls of the cups extend from the curvature of the individual structures diagonally outward, but never running in parallel along the long axis. Because of this growth formation, nanotube cups are intrinsically isolated from each other in a "stacked" conformation. This allows for the inherent separation of cups held together by van der Waals forces and an outer layer of amorphous carbon.

Mechanical separation, performed by grinding with a mortar and pestle, results in a black carbon powder of single nanotube cups. Figure 2 illustrates these separated cups and the structure they possess. As can be seen in Figure 2a, even though the cups are physically separated from one another, they tend to aggregate to-

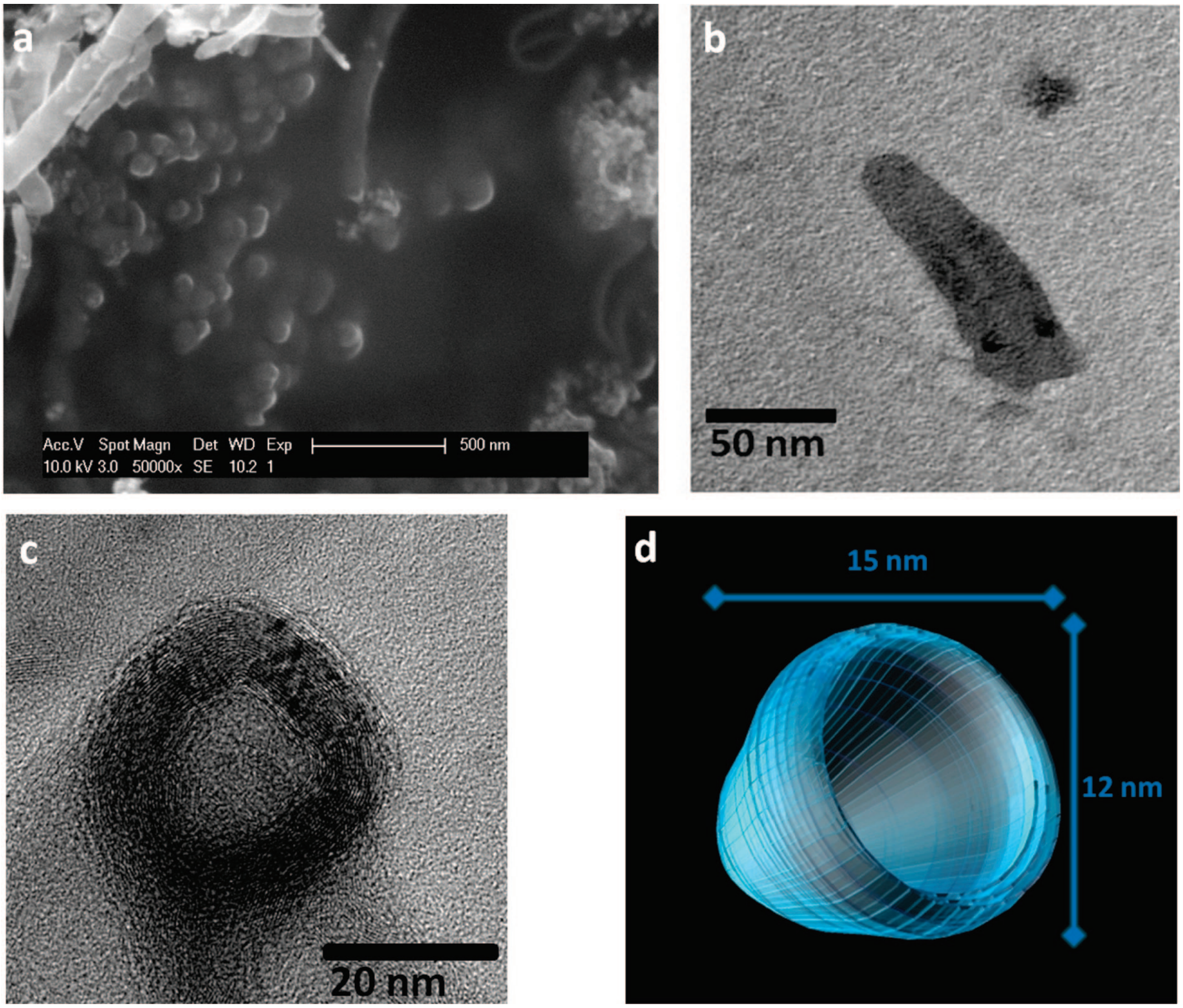

Figure 2. Separation of stacked cups. (a) SEM image of separated cups fixated to carbon tape. (b) Low resolution TEM image of a separated cup. (c) High resolution energy-filtered TEM image of a single, separated cup. (d) Translucent cartoon of a single, separated cup illustrating its multiple walls and hollow interior.

gether, presumably due to hydrogen bonding between each other through varying types of nitrogen functionalities located on their open rim. Figure 2 panels b and c further highlight the features of the cups, that is, the hollow interior and multiple walls (*ca.* 30 walls) encompassing the structure.

Individual nanotube cups, isolated as a black powder, are opened to further investigations using atomic force microscopy (AFM). Utilizing this technique provides valuable characterization, manipulation, and adhesion information.

Using AFM on a piece of freshly cleaved mica coated with 0.01% poly-L-lysine,[27] we could clearly distinguish cups as having a uniform height distribution narrowed to the range of 12−40 nm in height. Use of a sharp AFM probe (2−3 nm) is sufficient to map out the topology of the cups in terms of orientation on the treated mica surface. Figure 3a shows this conical orientation *via* a 3D topographical image. Furthermore, the phase image of Figure 3b depicts lighter portions in the center of the nanotube cup structure, indicative of a peak rather than a depression that would be seen if we were observing the open side of the cup. Presumably, amine and amide groups of poly-L-lysine, which can form hydrogen bonds with the nitrogen functionalities of nanotube cups, give this specific "open-side-down" orientation (Figure 3c). This orientation implies the presence of nitrogen atoms on the open edge of the cups, as was implicated in their growth mechanism.

Using the force of the tapping mode probe, we manipulated the cups across the mica surface by varying the force modulation. By increasing or decreasing the amplitude set point of the AFM, we can effectively extend or retract the tip to the mica surface.[28] This extension, therefore, acts as a means to mechanically manipulate the structures. We have observed that while nanotube cups easily move on an untreated mica surface (Supporting Information), they are strongly fixated to the poly-L-lysine treated mica surface (Figure 3d). As can be seen from the figure, the cups could be moved,

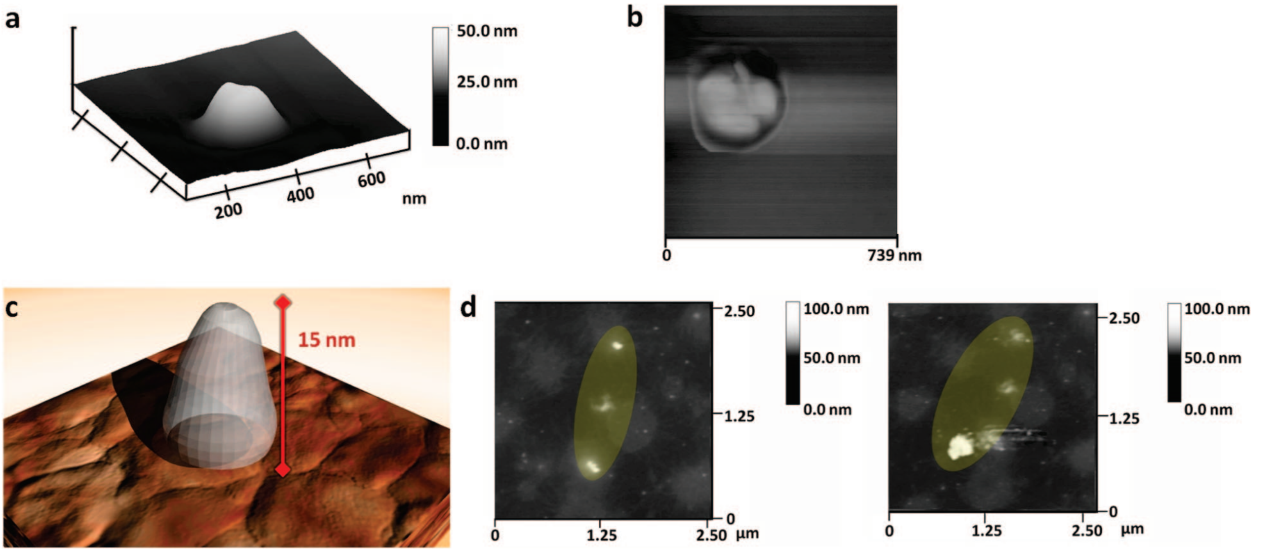

Figure 3. AFM characterization and manipulation of unmodified cups. (a) 3D AFM rendering of carbon nanotube cup oriented "open side" against a mica surface treated with poly-L-lysine (0.01%). (b) AFM phase image of carbon nanotube cup orientation. White color indicates peaks. (c) Translucent cartoon of a single nanotube cup oriented on a treated mica surface. (d) Mechanical manipulation of unmodified cup on treated mica surface.

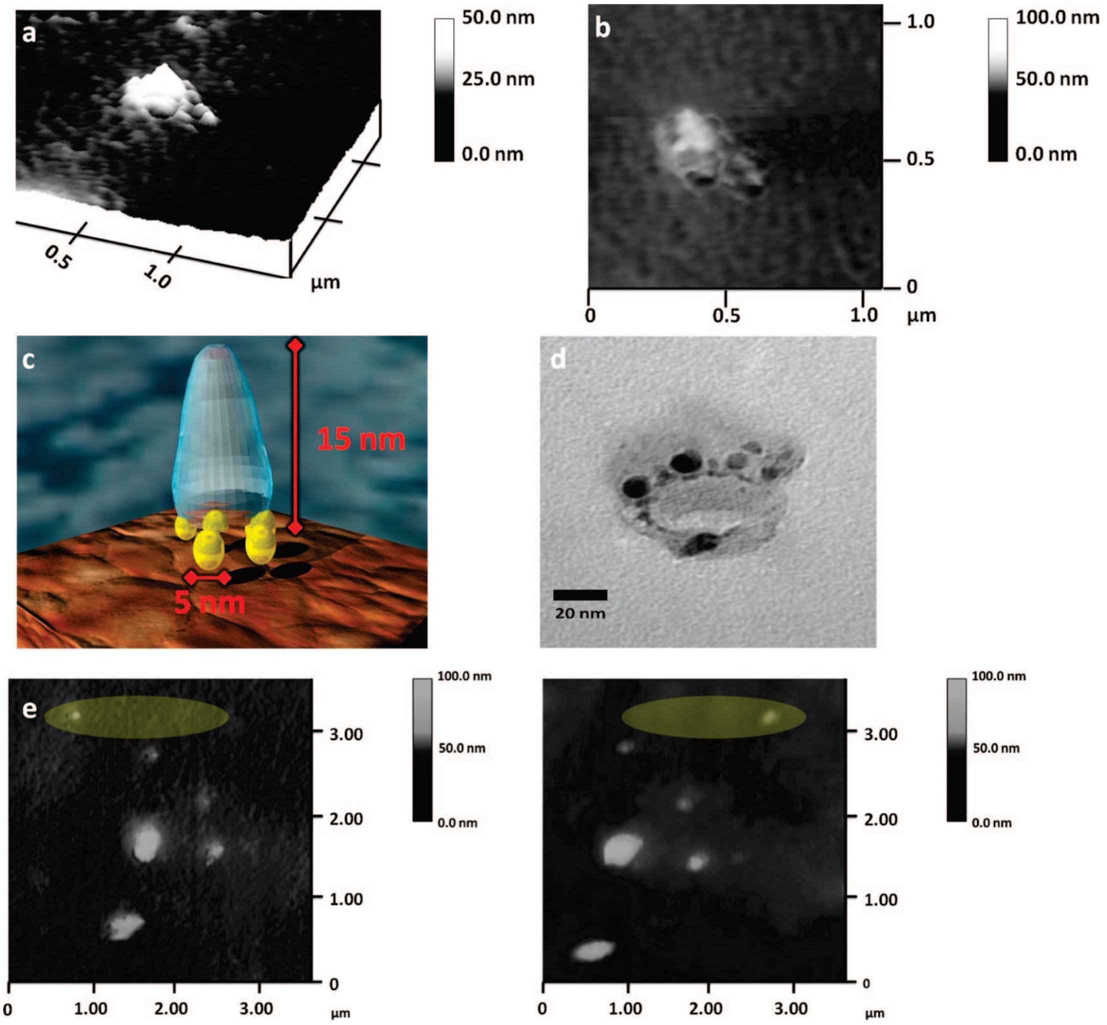

Figure 4. AFM characterization and manipulation of GNP-decorated cups. (a) 3D AFM rendering of a GNP-decorated, carbon cup on a treated mica surface. (b) AFM height image of GNP-decorated, carbon cup. Lighter portions indicate peaks. (c) Translucent cartoon indicating the decoration preference of GNPs on the open side of the cup structure. (d) Low resolution TEM image of a GNP-decorated carbon nanotube cup. (e) Mechanical manipulation of GNP-decorated cup on treated mica surface.

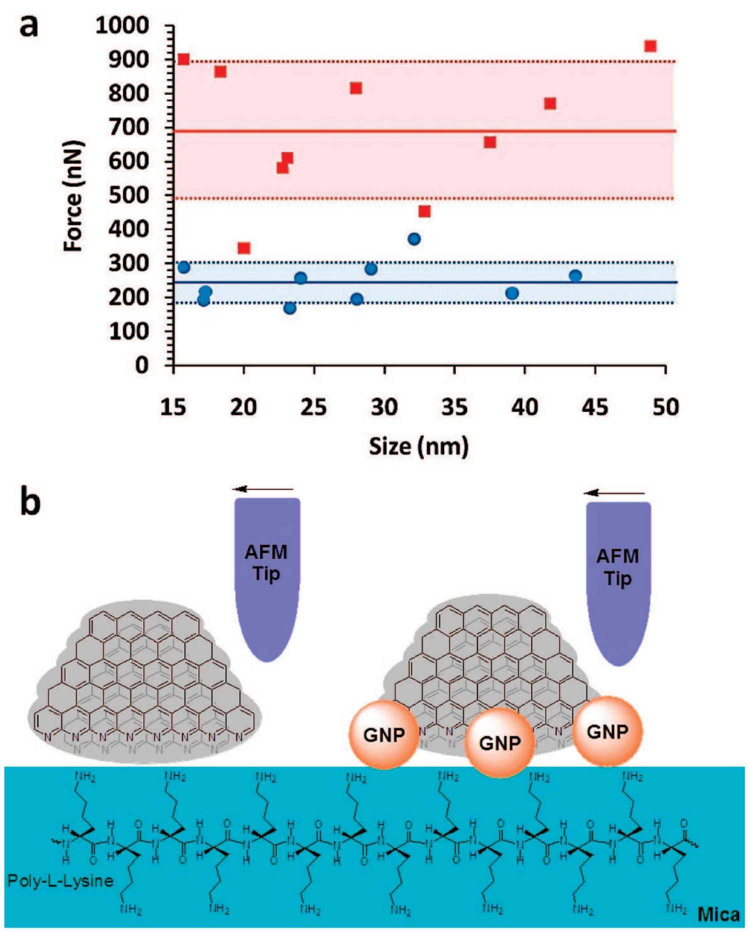

Figure 5. AFM experiment. (a) Comparison of adhesion forces *versus* cup's size for unmodified (■) and GNP-decorated (●) cups. Solid lines indicating average force and corresponding shaded areas (standard deviations) show statistically significant differences in adhesion of unmodified cups as compared to GNP-decorated cups. (b) Scheme demonstrating AFM manipulation experiment, where (left) mobility of unmodified cup is affected by hydrogen bonding between pyridine-like nitrogen functionalities on cup's edges and poly-L-lysine, and (right) improved by attachment of GNPs

however, only with excessive damage. In addition to the proposed hydrogen bonding, another source deterring nanotube cup movement in this orientation could be tribological processes occurring between the mica surface and the open side of the carbon nanotube cups.[29] Optimum adhesion forces, that is, friction, occurs when then the contacting surfaces perfectly conform to each other during the critical moment of pull-off, or when the tip forces movement to occur.[30] That being stated, we must assume that while there may not be perfect conformity between these two surfaces, even partial conformity must contribute to the determent of movement. Additionally, it also must be included that nitrogen doping within the interior lattice structure causes inherent defects, thus weakening the overall mechanical stability of the nanotube cup.[31,32]

To defer this fixation through hydrogen bonding on a hydrophilic surface, we sought to modify these basal nitrogen groups with gold nanoparticles. Through biotinylation of carbon nanotube cups and the corresponding reaction with streptavidin-coated GNPs, we were able covalently decorate the open edge of the cups. Cups were reacted with (+)-Biotin *N*-hydroxy-succinimide ester in *N*,*N*-dimethylformamide (DMF) at room temperature. After resuspending this complex into a 10% ethanol solution, we were able to combine streptavidin-coated GNPs in buffered solution to incubate. Following complete incubation (typically 24 h), we further characterized and manipulated the hybrid product *via* AFM in tapping mode. Figure 4 panels a and b show the topology of GNP-decorated cups. We can see the general structure is maintained by a single cup in the center surrounded by GNPs decorating the exterior, open-edge. We further visualize this by a low-resolution TEM image shown in Figure 4d. It is evident that the GNPs only decorate this open edge of the carbon nanotube cup, as approximately five GNPs of 10 nm or less are visible.

Additionally, as this sample was negatively stained with 2% uranyl acetate for improved contrast,[33] we can still see the streptavidin surrounding the materials. Incomplete biotinylation may have been responsible for the nonuniform distribution of GNPs around the exterior edge. Further section analysis of this self-complexed structure can be found in the Supporting Information. Incubation of unmodified cups with streptavidin-coated GNPs results in a lesser degree of attachment, presumably due to hydrogen bonding between streptavidin and the cups' nitrogen functionalities (Supporting Information). Therefore, biotinylation of cups is essential for GNP attachment.

Using the aforementioned parameters for tapping mode manipulation, we proceeded to determine whether we had deterred the fixation of cups through hydrogen bonding to a treated mica surface by the simple covalent attachment of GNPs. Figure 4e illustrates the manipulation of GNP-decorated cups using the same conditions as listed above. As observed from this image, it is quite evident that the modified cup is now free to be manipulated through probe force. In addition, it is seen that there is no structural deformation upon manipulation, indicating that the hydrogen bonding and tribological effects between sample and substrate have indeed been minimized.

To quantitatively measure the impact of adhesion through hydrogen bonding and subsequent determent through modification, force plots[34] in contact mode on the AFM were performed. The spring constant of our contact mode probe was first calculated using reference cantilevers (see Supporting Information). Surface images were then resolved in contact mode, prior to switching over to "force calibrate" mode to acquire a deflection sensitivity. It is important to note that the deflection sensitivity measurement was accurate as long as the laser spot position was not changed, that is, for the current sample. After acquiring this value (typically ~240 nm/V), the AFM was set to force volume mode where 10 force measurements were made on cups both unmodified and decorated each (see Supporting Information). Adhesion forces could thus be calculated using values obtained from force volume plots, as well as the deflection sensitivity, and spring constant. Figure 5a correlates adhesion forces for both unmodified and decorated cups. As can be seen there is no correlation between cup size and adhesion forces. Furthermore, it is evident that far less adhesion forces are involved in GNP-decorated cups. While force plots typically measure interactions between the sample and tip, we have already shown that cups have the same orientation regardless of modification. In these instances, a silicon probe is interacting with the graphitic, conical shell of the cup (Figure 5b). Only basal modification is imparted to these structures, indicating any variations in adhesion forces must be a result of sample/substrate interactions. Because of the presence of GNPs, there is a decrease in tribological effects as well as hydrogen bonding through passivated nitrogen groups of the cups.

CONCLUSIONS

To conclude, we have shown the synthesis of a versatile material and subsequent characterization and AFM manipulation. By showing that these structures have nitrogen atoms and can indeed be utilized for assembly opens up venues for many alternatives for this material. Decoration of cups with GNPs in this manner exploits the nitrogen groups on the exterior of these structures, a versatile point for "capping". By using the hollow interior for drugs and capping the structures through the amide linkage, it may be possible to create a nanoscopic delivery platform. Additionally, because of their "cuplike" shape, these structures can be used for nanocontainers, isolating reactions within their interior. With further exploration into this structure and "bottom-up" assembly, we can truly realize the full potential of these nanostructures in electronics, energy, biomedical, and chemical applications.

MATERIALS AND METHODS

Chemical Vapor Deposition Growth and Separation of Carbon Nanotube Cups. Cups were grown using the technique of CVD with a liquid precursor. Briefly, a Lindberg/Blue tube furnace was utilized at 950 °C. Using a three-foot long, sealed quartz tube (2.5 cm i.d.), cups were made by passing a liquid precursor consisting 5.0 g of MeCN, 1.25 g of ferrocene, and 93.75 g of EtOH at a rate of 5 mL/h for 1 hour. Carrier gases included Ar at 422 sccm and H_2 at 125 sccm. After 1 hour, the furnace, liquid injector, and H_2 gas were terminated, allowing for a 1 h cool down time in an argon atmosphere. The cup film was then collected off a quartz plate using a one-sided razor blade.

Separation of the stacked, as-prepared cups was done following the previously reported procedure.[19] The cup film was placed in a mortar and ground with a pestle along with a dropwise addition of EtOH. This grinding motion allowed for the physical separation of cups by breaking the van der Waals attraction between them. The solvent was then allowed to evaporate, and the solid product was collected for future use.

Decoration of Cups with Gold Nanoparticles. Approximately 1 mg of separated cups was suspended in DMF (Sigma Aldrich) *via* ultrasonication for approximately 20 min. After a stable suspension was formed this was allowed to react with an excess of 5 mM (+)-Biotin *N*-hydroxy-succinimide ester (Sigma Aldrich) in DMF for 24 h at room temperature. The suspension was then centrifuged at 3400 rpm for 20 min. Supernatant was discarded, and the cup−biotin complex was resuspended in 10% ethanol *via* ultrasonication.

Streptavidin (*from Streptomyces avidinii*)-coated gold nanoparticles (~10 nm nominal) in buffered aqueous glycerol solution were purchased from Sigma Aldrich. This concentrated sample was then diluted 100× with deionized water. The reaction between the streptavidin coated nanoparticles and cup−biotin complex was allowed to occur by mixing them at a ratio of 1:100 (cups to GNPs). We found best results occurred when incubation occurred at room temperature.

Characterization. The SEM images were obtained with a Philips XL-30 FEG microscope. The electron beam accelerating voltage of the SEM was held at 10.0 keV for all images. The cup samples, both as-prepared and separated, we probed as a powder fixated on to carbon tape without any heavy metal coating.

Low-resolution TEM images were obtained with a Philips/FEI Morgagni microscope. The electron beam accelerating voltage of the TEM was held at 80.0 keV for all imaging. All cup samples were prepared by suspension in DMF or EtOH and drop casting on a lacey carbon TEM grid (Pacific Grid-Tech) and by allowing the solvent to evaporate completely. For imaging of streptavidin/cup bioconjugates, samples were stained with 2% uranyl acetate for improved contrast. Stain was dropped on the sample and grid and allowed to dry for 10 min before excess stain was blotted away with filter paper.

High-resolution TEM images were obtained with a JEOL JEM-2100F field-emission microscope. The electron beam accelerating voltage of the HRTEM was held at 200 keV for all imaging. Energy filtering was performed for zero-point energy loss. All sample preparation remained the same as with the low-resolution microscope.

AFM characterization was carried out on a multimode scanning probe microscope (Veeco). Tapping mode with super sharp tips (AppNano ACL-SS) allowed for intricate manipulation and characterization.

Characterization of separated cups was carried out by freshly cleaving mica with double-sided tape. An aqueous solution of 0.01% poly-L-lysine (20 μL) was spin-coated on the mica at 100 000 rpm for one minute, followed by washing with an equal amount of deionized water. This was then allowed to dry for 45 min before spin coating one drop of cups suspended in DMF or, in the case of decorated cups, suspended in 10% EtOH. After all solvent evaporated, this was then characterized *via* tapping mode at a scan rate of 2.98 Hz and a drive frequency of 187.630 kHz.

Acknowledgment. The microscopy work was performed using the resources of NanoScale Fabrication and Characterization Facility (NFCF) and the Department of Materials Science and Engineering, University of Pittsburgh.

Supporting Information Available: A detailed description can be found of spring constant calculations, force volume plots, adhesion force calculations, and statistical data. This material is available free of charge *via* the Internet at http://pubs.acs.org.

REFERENCES AND NOTES

1. Kroto, H. W.; Heath, J. R.; O'Brien, S. C.; Curl, R. F.; Smalley, R. E. C_{60}: Buckminsterfullerene. *Nature* **1985**, *318*, 162–163.

2. Iijima, S. Helical Microtubules of Graphitic Carbon. *Nature* **1991**, *354*, 56–58.
3. Ugarte, D. Curling and Closure of Graphitic Networks under Electron-Beam Irradiation. *Nature* **1992**, *359*, 707–709.
4. Krishman, A.; Dujardin, E.; Treacy, M. M. J.; Hugdahl, J.; Lynum, S.; Ebbesen, T. W. Graphitic Cones and the Nucleation of Curved Carbon Surfaces. *Nature* **1997**, *388*, 451–454.
5. Iijima, S.; Yudasaka, M.; Yamada, R.; Bandow, S.; Suenaga, K.; Kokai, F.; Takahashi, K. Nano-Aggregates of Single-Walled Graphitic Carbon Nano-Horns. *Chem. Phys. Lett.* **1999**, *309*, 165–170.
6. Zhang, G. Y.; Jiang, X.; Wang, E. G. Self-Assembly of Carbon Nanohelices: Characteristics and Field-Emission Properties. *Appl. Phys. Lett.* **2004**, *84*, 2646–2648.
7. Hasobe, T.; Fukuzumi, S.; Kamat, P. V. Stacked-Cup Carbon Nanotubes for Photoelectrochemical Solar Cells. *Angew. Chem., Int. Ed.* **2006**, *45*, 755–759.
8. Novoselov, K. S.; Jiang, D.; Schedin, F.; Booth, T. J.; Khotkevich, V. V.; Morozov, S. V.; Geim, A. K. Two-Dimensional Atomic Crystals. *Proc. Nat. Acad. Sci.U.S.A.* **2005**, *102*, 10451–10453.
9. Rao, C. N. R.; Cheetham, A. K. Science and Technology of Nanomaterials: Current Status and Future Prospects. *J. Mater. Chem.* **2001**, *11*, 2887–2894.
10. Lee, S.; Pérez-Luna, V. H. Surface-Grafted Hybrid Material Consisting of Gold Nanoparticles and Dextran Exhibits Mobility and Reversible Aggregation on a Surface. *Langmuir* **2007**, *23*, 5097–5099.
11. Broz, P.; Driamov, S.; Ziegler, J.; Ben-Haim, N.; Marsch, S.; Meier, W.; Hunziker, P. Toward intelligent nanosize bioreactors: A pH-Switchable, Channel-Equipped, Functional Polymer Nanocontainers. *Nano Lett.* **2006**, *6*, 2349–2353.
12. Leonhardt, A.; Mönch, I.; Meye, A.; Hampel, S.; Büchner, B. Synthesis of Ferromagnetic Filled Carbon Nanotubes and their Biomedical Application. *Adv. Sci. Technol.* **2006**, *49*, 74–78.
13. Meunier, V.; Krstić, P. S. Enhancement of the Transverse Conductance in DNA Nucleotides. *J. Chem. Phys.* **2008**, *128*, 041103-1–041103-4.
14. Weda, P.; Trzebicka, B.; Dworak, A.; Tsvetanov, Ch. B. Thermosensitive Nanospheres of Low-Density Core—An Approach to Hollow Nanoparticles. *Polymer* **2008**, *49*, 1467–1474.
15. Ye, X.; Gu, X.; Gong, X. G.; Shing, T. K. M.; Liu, Z.−F. A Nanocontainers for the Storage of Hydrogen. *Carbon* **2007**, *45*, 315–320.
16. Bai, X. D.; Zhong, D.; Zhang, G. Y.; Ma, X. C.; Liu, S.; Wang, E. G.; Chen, Y.; Shaw, D. T. Hydrogen Storage in Carbon Nitride Nanobells. *Appl. Phys. Lett.* **2001**, *79*, 1552–1554.
17. Zhong, D. Y.; Zhang, G. Y.; Liu, S.; Wang, E. G.; Wang, Q.; Li, H.; Huang, X. J. Lithium Storage in Polymerized Carbon Nitride Nanobells. *Appl. Phys. Lett.* **2001**, *79*, 3500–3502.
18. Ma, X.; Wang, E.; Zhou, W.; Jefferson, D. A.; Chen, J.; Deng, S.; Ningsheng, X.; Yuan, J. Polymerized Carbon Nanobells and their Field-Emission Properties. *Appl. Phys. Lett.* **1999**, *75*, 3105–3107.
19. Ma, X.; Wang, E. G.; Tilley, R. D.; Jefferson, D. A.; Zhou, W. Size-Controlled Short Nanobells: Growth and Formation Mechanism. *Appl. Phys. Lett.* **2000**, *77*, 4136–4138.
20. Endo, M.; Kim, K. A.; Hayashi, T.; Fukai, Y.; Oshida, K.; Terrones, M.; Yanagisawa, T.; Higaki, S.; Dresselhaus, M. S. Structural Characterization of Cup-Stacked-Type Nanofibers with an Entirely Hollow Core. *Appl. Phys. Lett.* **2002**, *80*, 1267–1269.
21. Kim, C.; Kim, Y. J.; Kim, Y. A.; Yanagisawa, T.; Park, K. C.; Endo, M.; Dresselhaus, M. S. High Performance of Cup-Stacked-Type Carbon Nanotubes as a Pt-Ru Catalyst Support for Fuel Cell Applications. *J. Appl. Phys.* **2004**, *96*, 5903–5905.
22. Endo, M.; Kim, Y. A.; Ezaka, M.; Osada, K.; Yanagisawa, T.; Hayashi, T.; Terrones, M.; Dresselhaus, M. S. Selective and Efficient Impregnation of Metal Nanoparticles on Cup-Stacked-Type Carbon Nanofibers. *Nano Lett.* **2003**, *3*, 723–726.
23. Zhao, G. L.; Bagayoko, D.; Wang, E. G. Electronic Structure of Short Carbon Nanobells. *Mod. Phys. Lett. B* **2003**, *17*, 375–382.
24. Sun, H. -L.; Jia, J. -F.; Zhong, D.; Shen, Q. -T.; Sun, M.; Xue, Q. K.; Wang, E. G. Scanning Tunneling Microscopy Study of Polymerized Carbon Nanobells: Electronic Effect and Evidence of Nitrogen Incorporation. *Phys. Rev. B* **2002**, *66*, 085423−1085423−5.
25. Iijima, S.; Ichihashi, T.; Ando, Y. Pentagons, Heptagons and Negative Curvature in Graphite Microtubule Growth. *Nature* **1992**, *356*, 776–778.
26. Lin, M.; Ying Tan, J. P.; Boothroyd, C.; Loh, K. P.; Tok, E. S.; Foo, Y.-L. Dynamical Observation of Bamboo-Like Carbon Nanotube Growth. *Nano Lett.* **2007**, *7*, 2234–2238.
27. Chen, L.; Cheung, C. L.; Ashby, P. D.; Lieber, C. M. Single-Walled Carbon Nanotube AFM Probes: Optimal Imaging Resolution of Nanoclusters and Biomolecules in Ambient and Fluid Environments. *Nano Lett.* **2004**, *4*, 1725–1731.
28. Decossas, S.; Mazen, F.; Baron, T.; Brémond, G.; Souifi, A. Atomic Force Microscopy Nanomanipulation of Silicon Nanocrystals for Nanodevice Fabrication. *Nanotechnol.* **2003**, *14*, 1272–1278.
29. Dietzel, D.; Mönninghoff, T.; Jansen, L.; Fuchs, H.; Ritter, C.; Schwarz, U. D.; Schirmeisen, A. Interfacial Friction obtained by Lateral Manipulation of Nanoparticles using Atomic Force Microscopy Techniques. *J. Appl. Phys.* **2007**, *102*, 084306-1–084306-11.
30. Muto, H.; Yamada, K.; Miyajima, K.; Mafuné, F. Estimation of Surface Oxide on Surfactant-Free Gold Nanoparticles Laser-Ablated in Water. *J. Phys. Chem.* **2007**, *111*, 17221–17226.
31. Sumpter, B. G.; Meunier, V.; Romo-Herrera, J. M.; Cruz-Silva, E.; Cullen, D. A.; Terrones, H.; Smith, D. J.; Terrones, M. Nitrogen-Mediated Carbon Nanotube Growth: Diameter Reduction, Metallicity, Bundle Dispersability, and Bamboo-like Structure Formation. *ACS Nano* **2007**, *1*, 369–375.
32. Panchakarla, L. S.; Govindaraj, A.; Rao, C. N. R. Nitrogen- and Boron-Doped Double-Walled Carbon Nanotubes. *ACS Nano* **2007**, *1*, 494–500.
33. Wu, Y.; Hudson, J. S.; Lu, Q.; Moore, J. M.; Mount, A. S.; Rao, A. M.; Alexov, E.; Ke, P. C. Coating Single-Walled Carbon Nanotubes with Phospholipids. *J. Phys. Chem. B* **2006**, *110*, 2475–2478.
34. Willing, G. A.; Ibrahim, T. H.; Etzler, F. M.; Neuman, R. D. New Approach to the Study of Particle-Surface Adhesion using Atomic Force Microscopy. *J. Colloid Interface Sci.* **2000**, *226*, 185–188.